Numerical Investigation of Influence of Cavity Air Injection Panels in Ultra-Compact Combustor

Ujjwal Tiwari[*], Hao Tang [**], Anh Tu Dang [***]

*,**,*** *Nanjing University of Aeronautics and Astronautics, Jiangsu Province Key Laboratory of Aerospace Power System, Nanjing 210016, China*

DOI: 10.29322/IJSRP.9.04.2019.p8897
http://dx.doi.org/10.29322/IJSRP.9.04.2019.p8897

Abstract- Ultra-Compact combustion presents an innovative solution to address the demand for increasingly compact, efficient, and low weight aircraft gas turbine engine propulsion systems. An Ultra-Compact Combustor (UCC) operates by diverting a portion of the compressor exit flow into a cavity about the engine outer diameter. Injection into the cavity can be done at an angle to induce bulk circumferential swirl. Swirl velocities in the cavity then impart a centrifugal load of approximately $1000g_0$.
Computational results from the test rig are presented, prioritizing on establishing the design flow split through the diffuser into the circumferential cavity. The implementation of a core channel plate was instrumental in control of the mass flow splits. Computational Fluid Dynamics (CFD) supplement the experiments and enable a more detailed understanding of the interactions within the diffuser and the interactions between the air injection jets and the fuel jets. Three different conditions of cavity air flow rate were studied by changing the diameter of the cavity air injection panels three times respectively. The results show that the dimension of cavity air injection panels is directly related to the centrifugal acceleration of the gas mixture in the combustion ring. The panels with the smallest diameter achieved the highest combustion temperature in the cavity. Varying the diameters of cavity air injection panels with respect to core channel restriction plate caused a change in the core flow development which then had a secondary effect of aiding the combustion process within the cavity.

Index Terms- Analysis, Cavity air injection panels, Computational Fluid Dynamics, Ultra-Compact Combustor

I. INTRODUCTION

The traditional jet engine combustor is axial in flow. The compressor diffuses the air as it leaves the compressor, so the flow is at a low Mach number when entering the combustor, where fuel is introduced to the airflow, mixed, and burned. The hot combusted gas is then sent to the turbine to be transferred into work to power the compressor and the electrical systems of the aircraft. The combustor must be long enough for the air-fuel mixture to burn completely before entering the turbine. An alternative to the traditional combustor is the Ultra-Compact Combustor (UCC) which performs the combustion process in the circumferential direction. The UCC utilizes the circumferential direction to create the needed residence time for combustion, while effectively reducing the overall length of the combustor. The centripetal acceleration in the cavity causes a g-load effect in the cavity. This concept has been termed an Ultra-Compact Combustor, and it is illustrated in Figure 1 through comparison with a traditional combustor.

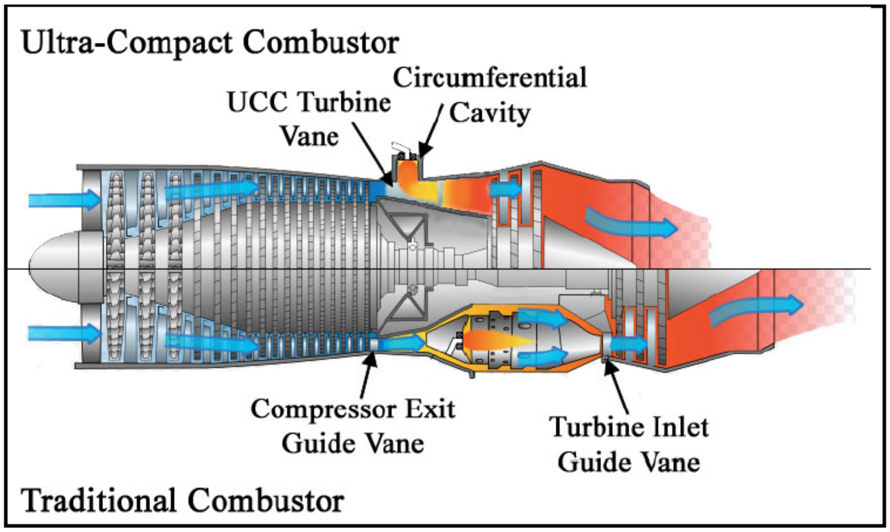

Figure 1: Axial length comparison of traditional and Ultra-Compact Combustors

II. BACKGROUND

In 1973, Lewis [1] first proposed the theory of centrifugal combustion to accelerate the flame propagation velocity. Zelina et al. [2] experimentally confirmed that the ultra-compact combustion chamber flame length is at least 50% shorter than the conventional combustion chamber. Sirignano et al. [3] analytically demonstrated the benefits to engine cycle performance realized through the addition of inter-turbine combustion stages. In recent years, The US Air Force Research Laboratory (AFRL) has further explored the practical application of ultra-compact combustors. In 2013, Bohan and Polanka [4] designed a full-scale (fighter-sized) computational UCC model to quantify performance with non-reacting and reacting air. Their work also resulted in the foundation for the current "hybrid vane" design incorporated in the UCC core flow. The hybrid vane fulfills the roles of both the compressor exit guide vane and the turbine inlet guide vane, thereby further capitalizing on the ability of the UCC to reduce overall engine length and complexity. The combustion cavity circles above the vane, therefore the hybrid vane plays a crucial role in the recombination of the combusted cavity flow and the core through-flow. In 2013, Wilson [5][6] proposed a low Rayleigh loss centerbody design of the UCC.

For the first time in 2013, Conrad [7][8] improved the direction of core and cavity air flow intake, realized axial and radial intake of core and cavity flow, effectively reduced the radial scale of ultra-compact combustion chamber, and significantly promoted the practical application of UCC. Conrad developed a new annular UCC rig that diverts the axial airflow by adding a diffuser in front of the combustion ring and arranging the cavity air injection panels obliquely in the front wall of the combustion ring to ensure swirling combustion in the combustion ring. In 2014, Miranda [9] based on the Conrad experimental device and using hybrid vanes for experimental research, it was expected to achieve core-to-cavity mass flow distribution 60/40, 70/30, 80/20 by changing the core and cavity flow area ratio. Both Conrad [7] and Miranda [9] found that it was difficult to drive the desired mass flow rate into the circumferential cavity due to the relative pressures between the core and cavity flow paths. There were minimal restrictions to the core flow, whereas the cavity flow was diverted through a narrow channel and forced through a series of small injection holes in the air driver plates. The injector plate caused a pressure drop that was not seen by the core flow and resulted in a lower than expected mass flow rate into the cavity for each of the middle diameter splits. Cottle et al. [10] were able to correct this problem using a flow restrictor plate located downstream of the support vanes in the diffuser core flow but before the hybrid vanes. The plate provided the necessary pressure drop in the core flow to allow the pressures between the two flow paths to behave predictably. With the addition of the flow restrictor plate back pressuring the core flow, the mass flow rate split was nearly matched to the diffuser split ratio. However, the entire flow field analysis is limited to the cold flow of the combustion chamber.

In the same year, Cottle and Polanka [11] conducted a numerical analysis to look at the velocity profile through the diffuser passage that leads to the circumferential cavity. They found that the velocity profile was not a typical parabolic channel flow profile with the maximum velocity in the center of the passage. Instead, they found that the maximum occurred at a non- dimensional height of 0.1. Additionally, at a channel height of 0.7 to 1.0 there was reversed flow in the passage. One possible cause of the irregular pattern could have been to the placement of the leading edge of the diffuser middle diameter ring. In Figure 3 it can be seen that the tip of the middle diameter ring is in-line with the OD of the air supply line creating a situation where it was difficult for the flow to remain attached to the outer wall as it diffused.

Sun Ming Shan [12] in 2018 performed numerical investigation of blockage plate in the UCC model of Conrad [7] and Miranda [9]. The results showed that the low-pressure area created by restriction plate enhances the radial flow migration and enforce the mixing ability between high-temperature gas and core flow, which benefits the performance of temperature profile in outlet plate. Moreover, the simulation results also concluded the restriction plate could enlarge the size of vortex that exists in the cavity ring and improve the stability of combustion. This current report will document the continuation of the numerical investigation of the restriction plate along with the air injection cavity flow.

III. COMPUTATIONAL METHODS

For the past decade, the Air Force Institute of Technology (AFIT) and the Air Force Research Laboratory (AFRL) have been investigating and advancing the development of an Ultra-Compact Combustor (UCC) as a means to improve efficiency and reduce the size of aircraft engines. The complete structure of the AFIT test rig of UCC is shown in Figure 2. It is mainly composed of a diffuser, a combustion ring, a restriction plate, and a center body. According to the sectional view of the combustion chamber, the air enters the combustion chamber through the inlet, and diffuser divides the airflow into a core flow and a cavity flow. The cavity flow is inclined at an angle into the combustion ring, mixed with the fuel injected from above the combustion ring, and then swirled and combusted. The diffuser support vanes guide the core flow, then passing through the core channel restriction plate to the circumferential cavity. The core flow then gets blended with the combustion ring products, which is then discharged along the hybrid guide vanes.

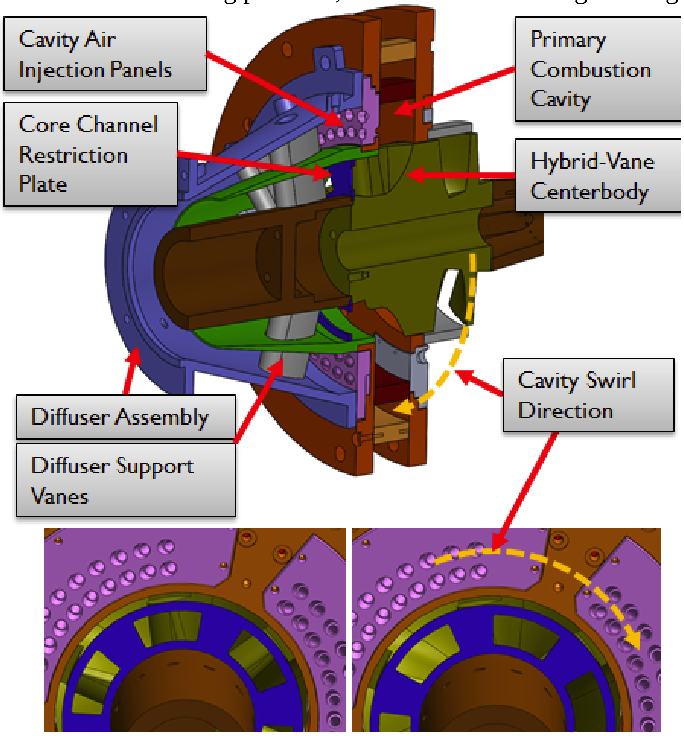

Figure 2: AFIT common-source hardware components (top) and restrictor plate detail “on-vane” (bottom-left) and “in-passage” (bottom-right)

A. Geometric Model

Siemens NX 11.0 was used to model the geometry of AFIT test rig. The total length of the combustion chamber is 449 mm; the diameter of the combustion ring is 159 mm. Location "D1" corresponds to a position roughly 30 mm downstream of the diffuser flow-split, while locations "C1" and "C2" are each about 5 mm from the fore and aft cavity sidewalls, respectively. The domain includes the full annulus (no periodic or symmetric boundaries).

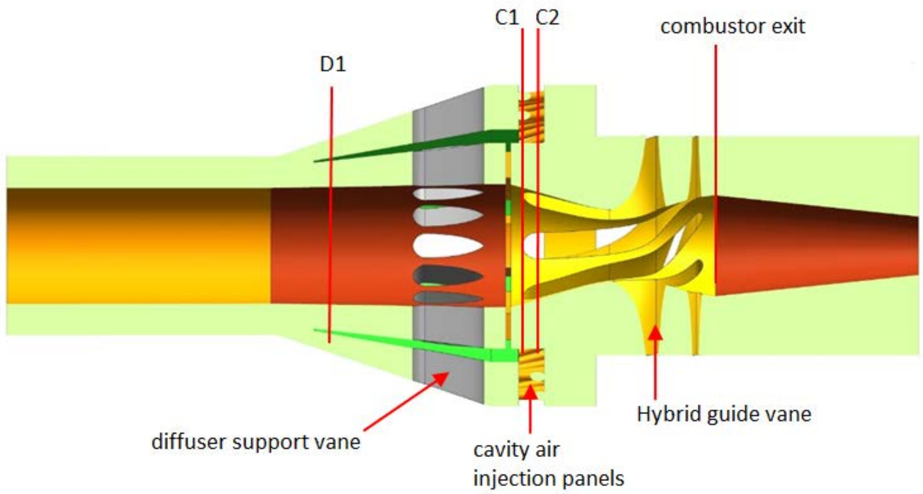

Figure 3: Axial reference positions

The outer passage of the diffuser directs the flow into the combustion cavity via cavity air injection panels. The nominal diameter of those holes in AFIT UCC is 4.5 mm. There are 60 such holes to guide the cavity airflow into the combustion cavity, angled at 30° relative to the engine axis.
Cottle [10] performed simulations using channel plate design of $\lambda = \{0.7, 1.0. 1.3\}$, where λ is a non-dimensional factor used to design the core blockage channel plate.

$$\frac{A_{channelPlate}}{A_{core}} = \frac{\lambda A_{injectionHoles}}{A_{cavity}}$$
$$A_{core} = \pi({r_{core,outer}}^2 - {r_{core,inner}}^2) = \pi R_c$$
$$A_{cavity} = \pi({r_{cavity,outer}}^2 - {r_{cavity,inner}}^2) = \pi R_v$$
$$A_{injectionHoles} = N\pi {r_h}^2, \text{where } r_h = radius\ of\ injection\ holes$$

$$A_{channelPlate} = \frac{6\phi\pi}{360}(r_1^2 - r_2^2)$$

From the model,

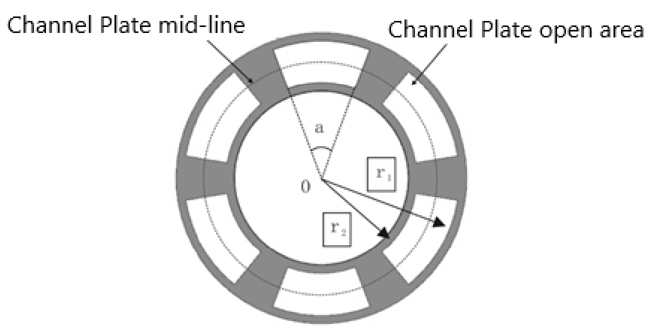

Figure 4: Core Blockage Channel Plate Schematic

$$\frac{12h^2}{\pi R_c} = \frac{\lambda N {r_h}^2}{R_v}$$

$$h = r_1 - r_2$$

So, keeping all the other parameters constant, values of r_h are calculated from the values of λ used by Cottle [10].

λ	$r_h(mm)$
0.7	2.5
1.0	2.25
1.3	2.0

So, three different cases with diameter of cavity air injection panels of 5.0 mm, 4.5 mm and 4.0 mm are used for simulation.

B. Computational Grid

Due to the complex geometry of the model, and considering the problem of computational accuracy caused by the periodic processing of the model, the model was divided into structured polyhedral mesh. During meshing, the model is divided into various details of the combustion chamber, such as fuel inlet, air inlet, wall, fluid regions, etc., and these areas are mesh-encrypted. The total number of cells is around 1.7 million.

Figure 5: UCC grid schematic

The flow solver used for this study was Fluent 18.0. The solver used the settings based on the recommendations of Mongia [13]. The turbulence model uses a realizable model with high accuracy in combustion chambers [14], and the normal wall function is used in near-wall areas where turbulence development is insufficient. The combustion model uses a component transport model, the reaction rate using eddy-dissipation model (EDM), and the combustion reaction using propane single-step reaction, such as equation (1):

$$C_3H_8 + 5O_2 \rightarrow 3CO_2 + 4H_2O$$

Separate implicit steady-state solver was used, and each discrete item adopted a second-order precision discrete format, which was calculated by SIMPLEC algorithm.

C. Boundary conditions and calculation parameters

Table 1: Boundary conditions of inlet and outlet

Parameter	**Value**
Inlet mass flow rate/(kg/s)	0.12
Inlet flow T/K	293
Operating pressure/Pa	101325
Inlet Gauge pressure/Pa	0
Oxygen mass fraction of inlet flow/%	23

Outlet T/K	293
Outlet Gauge Pressure/Pa	0

The equivalence ratio of the combustion ring is calculated based on the estimated cavity air flow rate of the diffuser design. The ratio of the inner and outer rings is 70/30, and the outer ring flow is calculated to be 0.036 kg/s. Fuel mass flow rate is 0.00158kg/s. The calculation conditions are shown in Table 2.

The effects of performance of the combustion chamber under different dimensions of air injection holes (diameter of 4.0 cm, 4.5 mm, and 5.0 mm) are considered.

IV. Calculation Results and Analysis

A. Influence of cavity air injection holes in cavity air flow rate and equivalence ratio

Table 2: Cavity air flow rate and equivalence ratio under different dimensions of air injection holes

Diameter of air injection holes	**4.0mm**	**4.5mm**	**5.0mm**
Fuel flow rate	0.001582(kg/s)	0.001582(kg/s)	0.001582(kg/s)
Cavity air flow rate	0.02511(kg/s)	0.03079(kg/s)	0.03416(kg/s)
Equivalence ratio	1.3696	1.1170	1.0677

It can be seen from Table 2 that the diameter of different cavity air injection holes directly affects the ratio of fuel to air in the combustion chamber. As the diameter of the air injection holes increases, the cavity air flow increases and the equivalence ratio decreases. In this case, the equivalence ratios are 1.370, 1.17, and 1.068 respectively.

ISSN 2250-3153

B. Analysis of results at D1 in combustion chamber

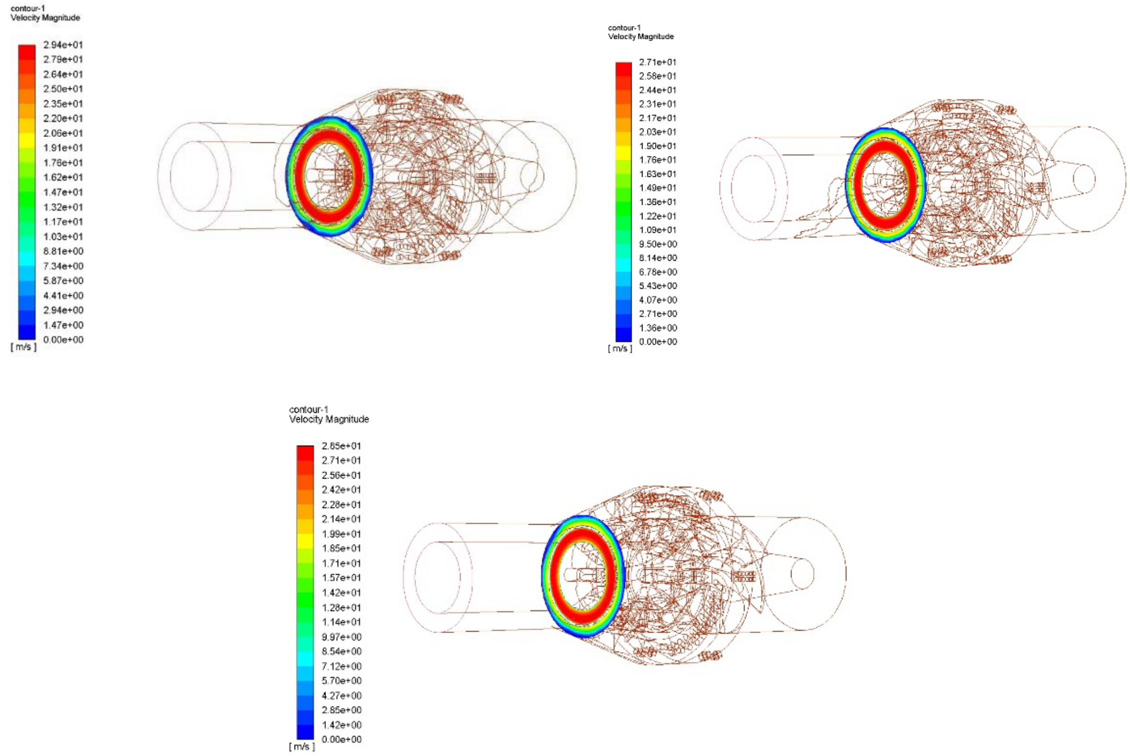

Figure 6: Tangential velocity contours at D1 when air injection holes have diameters 4.0mm, 4.5mm, and 5.0mm respectively

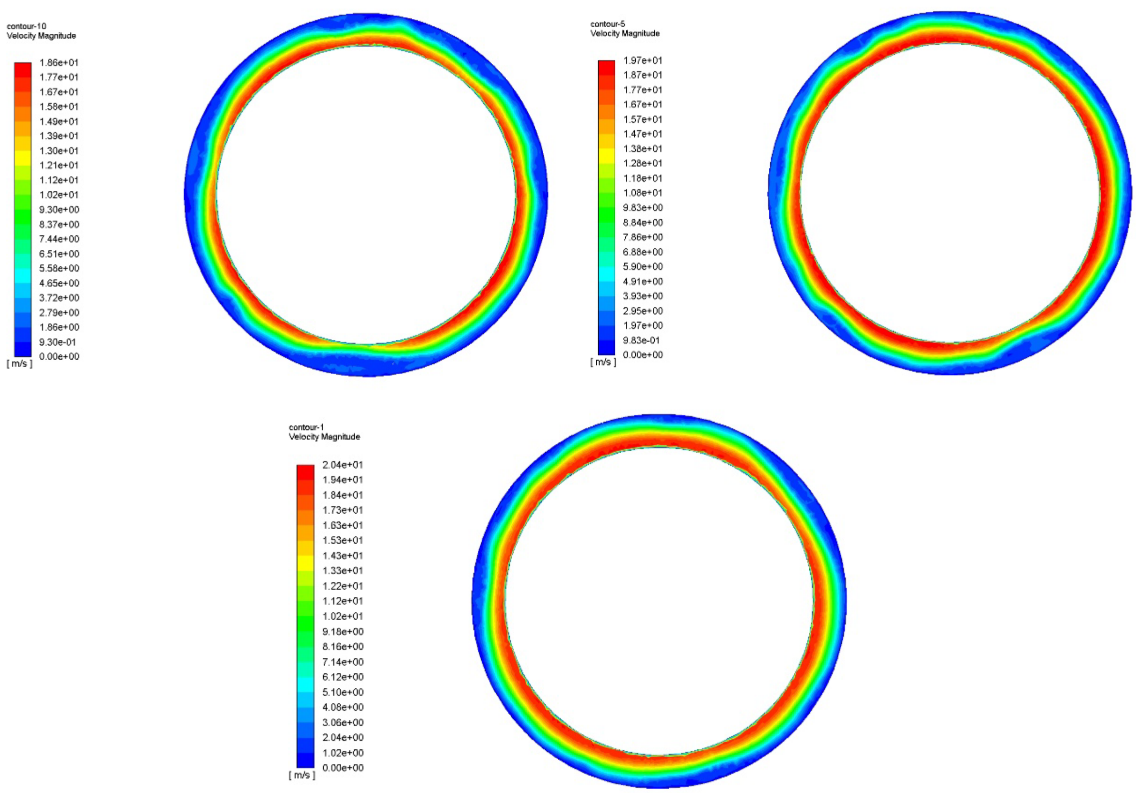

Figure 7: Tangential velocity contours at D1 cavity when air injection holes have diameters 4.0mm, 4.5mm, and 5.0mm respectively

It can be seen from Figure 6 and Figure 7 that the cross-section of the combustion chamber D1 is a concentric ring. Compared with the mainstream core flow, the velocity of cavity flow is lower due to the inclined inlet air flow rate. The velocity distribution of the cavity flow in the concentric ring is higher towards the inner ring. Since the diameter of cavity air injection panel affects the cavity flow rate, it also affects the air distribution into the combustion ring. Moreover, the maximum velocity in the cavity of the D1 section increases with the increase of the cavity flow rate.

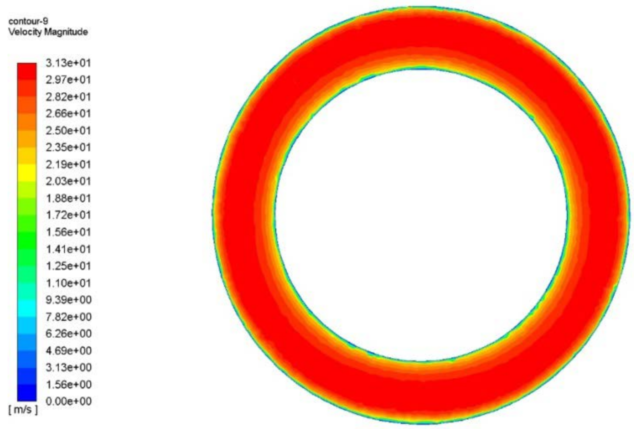

Figure 8: Tangential velocity contour at D1 core

The velocity distribution of the core flow exhibits an anti-U-shaped distribution. The velocity is lower at the two walls due to the viscosity and, rapidly increases along the radial direction as shown in Figure 8.

C. Analysis of results at D1 in combustion chamber

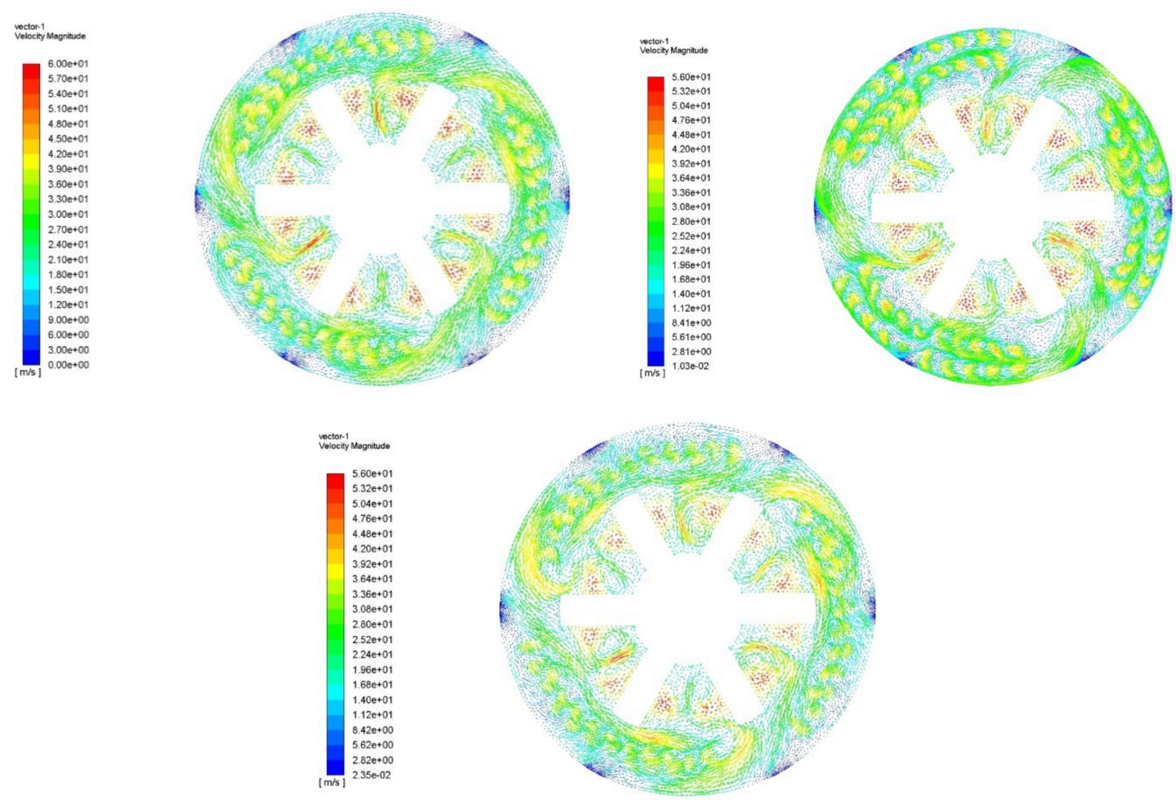

Figure 9: Vector velocity diagram of the cross-section velocity at C1 when air injection holes have diameters 4.0mm, 4.5mm, and 5.0mm respectively

It can be seen from Figure 9 that the velocity vector distribution of the air injection cavity holes of different diameters is similar at the C1 section in the combustion chamber, and the velocity at a position close to the fuel inlet is small. In the C1 section closer to the outer ring wall, due to the fuel and the cavity air, a combustion mixed gas vortex is formed in the combustion chamber, in which the fuel is mixed with the air and burned. Whereas in the C1 section closer to the inner wall, the gas after combustion of the fuel mixture is mixed with the mainstream air to form an air vortex to lower the temperature of the gas. As seen from the figure below, as the airflow rate in cavity increases, the overall velocity of the C1 section decreases slightly.

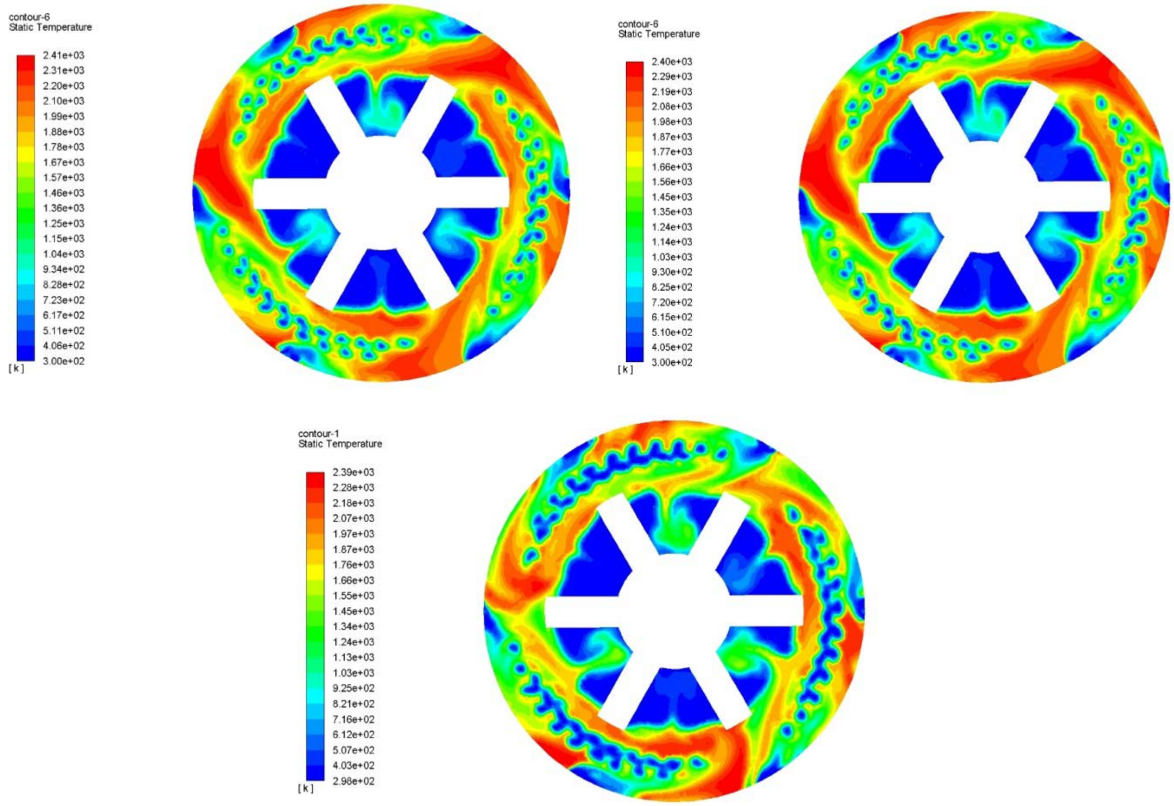

Figure 10: Temperature contours at C1 when air injection holes have diameters 4.0mm, 4.5mm, and 5.0mm respectively

Moreover, from figure 10, on the cross-section C1, the maximum combustion temperature is the highest when the equivalence ratio is the maximum. At the same time, it is found that for different diameters of air injection holes, the C1 section has different gas temperature distributions among the six-turbine blades, and the temperature between the three turbine blades is higher, the temperature is about 1200K to 1600K, and the other three turbine blades is lower, basically about 600K. Combined with the temperature distribution at the outlet of the combustion chamber, it can be found that the gas temperature distribution law between the six-turbine blades is similar to that of the C1 cross-section. The gas temperature between the three turbines is higher and is located in the radially middle of the outlet section, and the other three are close outside the outlet section.

D. Analysis of results at the outlet of combustion chamber

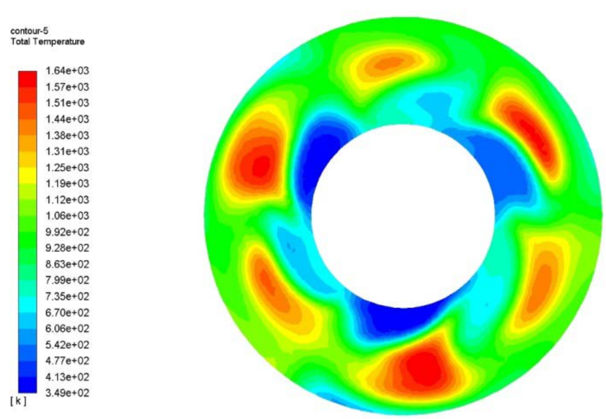

Figure 11: Temperature contours at outlet of combustion chamber when air injection holes have diameter of 4.0 mm

The temperature distribution at the outlet of the combustion chamber when cavity air injection holes have diameters of 4.0mm, 4.5mm and 5.0mm are presented by the graph in Figure 11.

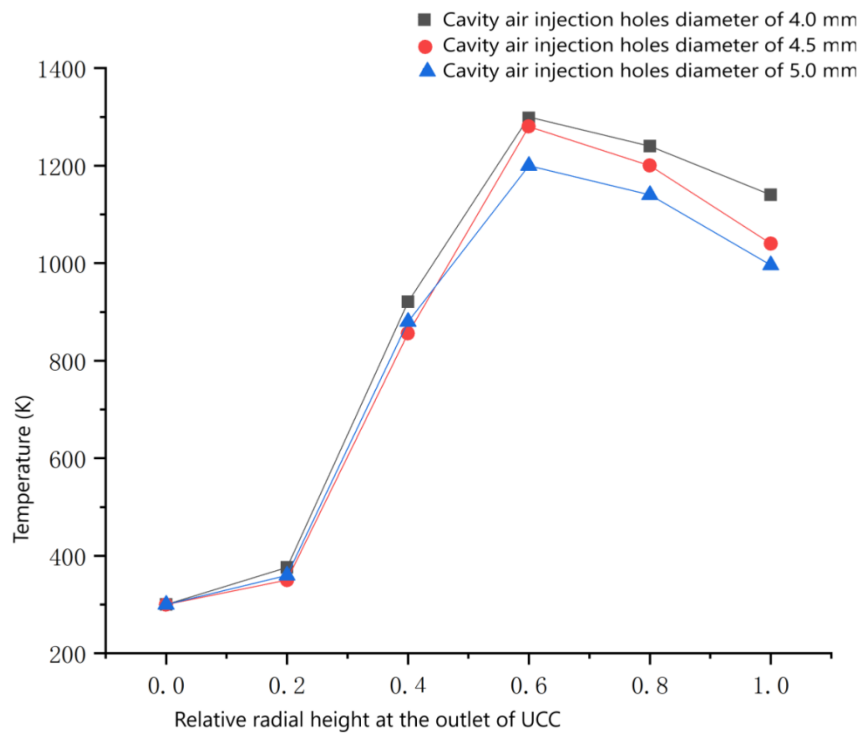

Figure 12: Average temperature at the outlet of the combustion chamber radially

It can be seen from Figures 11 and 12, that under different air injection holes conditions, the average temperature of the outlet at the time of combustion gradually decreases with the increase of the pore size. Moreover, the place where the temperature difference of the outlet section is the largest is at a relatively high radial height of the combustion chamber, that is, close to the outer wall of the combustor ring. In the inner wall, due to the small gas flow between the three blades between the turbine blades, the air flow mainly comes from the core flow, and the temperature is 300K. Therefore, the average radial temperature at the outlet is lower near the inner ring of combustion.

V. CONCLUSION

This paper presents the influence of the cavity air injection panels on the flow and combustion performance in the UCC. A combustor model was used to replicate the circumferential mixing utilized in UCC configurations to study the effects of centrifugal forces on combustion stability and efficiency. It is found that changing the diameter of cavity air injection panel changes the equivalence ratio of fuel to air, and at the same time affects the cavity and core air flow rate. The vector field in the combustion cavity changes, thereby affecting the combustion within the combustion ring. Reducing the diameter of the panel increases the combustion temperature in the cavity, providing evidence to the higher temperature in the outlet of the combustion chamber. However, a minimal diameter of the air injection panels might lead to insufficient airflow in the cavity, while delaying the combustion and decreasing the combustion efficiency, which needs further research in future.

ACKNOWLEDGMENT

This work was supported by the National Nature Foundation of China (91641131). The authors also gratefully acknowledge the generous allocation of computing time at the Jiangsu Province Key Laboratory of Aerospace Power System.

REFERENCES

[1] G. L.-S. (International) on Combustion and undefined 1973, "Centrifugal-force effects on combustion," *Elsevier*.

[2] J. Zelina, D. S.-… for Land, undefined Sea, and undefined 2004, "Ultra-compact combustors for advanced gas turbine engines,"

… *.asmedigitalcollection.asme.org*.

[3] W. A. Sirignano and F. Liu, "Performance Increases for Gas-Turbine Engines Through Combustion Inside the Turbine," *J. Propuls. Power*, vol. 15, no. 1, pp. 111–118, Jan. 1999.

[4] B. T. Bohan and M. D. Polanka, "Analysis of Flow Migration in an Ultra-Compact Combustor," *J. Eng. Gas Turbines Power*, vol. 135, no. 5, p. 051502, Apr. 2013.

[5] J. D. Wilson and M. D. Polanka, "Reduction of Rayleigh Losses in a High G-Loaded Ultra Compact Combustor," in *Volume 1A: Combustion, Fuels and Emissions*, 2013, p. V01AT04A057.

[6] J. Wilson, "Characterizing G-Loading, Swirl Direction, and Rayleigh Losses in an Ultra Compact Combustor," 2013.

[7] M. Conrad, J. Wilson, … M. P.-A. J., and undefined 2013, "Integration issues of an Ultra-Compact Combustor to a jet turbine engine," *arc.aiaa.org*.

[8] M. M. Conrad, "Integration of an Inter Turbine Burner to a Jet Turbine Engine." 2013.

[9] J. L. Miranda and M. D. Polanka, "The Use of an Ultra-Compact Combustor as an Inter-Turbine Burner for Improved Engine Performance," in *52nd Aerospace Sciences Meeting*, 2014.

[10] A. Cottle and M. D. Polanka, "Optimization of Ultra Compact Combustor Flow Path Splits," no. January, pp. 1–11, 2015.

[11] A. Cottle, M. P.-A. Turbo, and undefined 2016, "Numerical and experimental results from a common-source high-g ultra-compact combustor," … *.asmedigitalcollection.asme.org*.

[12] 孙明山, "节流盘对超紧凑燃烧室性能影响的数值研究," 2018.
SUN Ming-shan , Numerical Investigation of Influence of Blockage Plate on Ultra Compact Combustor, 2018

[13] H. Mongia, "Recent Progress in Comprehensive Modeling of Gas Turbine Combustion," in *46th AIAA Aerospace Sciences Meeting and Exhibit*, 2008.

[14] Y. YONEZAWA, H. TOH, S. GOTO, and M. OBATA, "Development of the jet-swirl high loading combustor," in *26th Joint Propulsion Conference*, 1990.

AUTHORS

First Author – Ujjwal Tiwari, Postgraduate Student, Nanjing University of Aeronautics and Astronautics, tiwariujjwal@nuaa.edu.cn
Second Author – Hao Tang, Professor, Nanjing University of Aeronautics and Astronautics, hao.tang@nuaa.edu.cn
Third Author – Anh Tu Dang, Doctorate Student, Nanjing University of Aeronautics and Astronautics, danganhtukq@nuaa.edu.cn